

Impact of compressive in-plane strain on the ferroelectric properties of epitaxial NaNbO3 films on (110) NdGaO3

R. Wördenweber, J. Schwarzkopf, E. Hollmann, A. Duk, B. Cai et al.

Citation: Appl. Phys. Lett. 103, 132908 (2013); doi: 10.1063/1.4822328

View online: http://dx.doi.org/10.1063/1.4822328

View Table of Contents: http://apl.aip.org/resource/1/APPLAB/v103/i13

Published by the AIP Publishing LLC.

Additional information on Appl. Phys. Lett.

Journal Homepage: http://apl.aip.org/

Journal Information: http://apl.aip.org/about/about_the_journal Top downloads: http://apl.aip.org/features/most_downloaded

Information for Authors: http://apl.aip.org/authors





Impact of compressive in-plane strain on the ferroelectric properties of epitaxial NaNbO₃ films on (110) NdGaO₃

R. Wördenweber, $^{1,a)}$ J. Schwarzkopf, 2 E. Hollmann, 1 A. Duk, 2 B. Cai, 1 and M. Schmidbauer 2

¹Peter Grünberg Institute (PGI) and JARA-Fundamentals of Future Information Technology, Forschungszentrum Jülich, D-52425 Jülich, Germany

(Received 8 May 2013; accepted 10 September 2013; published online 25 September 2013)

Epitaxial a-axis oriented NaNbO $_3$ films are grown on (110) oriented NdGaO $_3$ substrates. The lattice mismatch between substrate and film leads to compressive strain of \sim 0.7% in the a-c plane. As a consequence, the in-plane permittivity and tunability are strongly enhanced compared to bulk NaNbO $_3$, and a pronounced maximum in the temperature dependence of the permittivity occurs. Below the maximum at $T_{max} \approx 250\,\mathrm{K}$, ferroelectric behavior is observed that seems to vanish above T_{max} . The pristine phase of the film at $T < T_{max}$ is antiferroelectric and is easily suppressed by small applied electric fields. The ferroelectric phase shows a relaxor type behavior. © 2013 AIP Publishing LLC. [http://dx.doi.org/10.1063/1.4822328]

In the last years, alkali niobates have attracted scientific interest due to their ferroelectric and piezoelectric properties that are comparable to lead-zirconate-titanate (PZT)-based material. Intensive studies on the fabrication of alkali niobate-based ceramics with large ferroelectric and piezoelectric properties have been carried out.² Among the family of alkali niobates, NaNbO3 and NaNbO3-based materials proved to be very promising candidates due to their complexity of phase transitions and their highly interesting electronic behavior especially under influence of an applied electric field.^{2,3} At room temperature, NaNbO₃ exhibits the antiferroelectric orthorhombic p-phase (space group Pbma). However, applying an electric field induces a phase transition to the ferroelectric phase (space group $P2_1ma$). At the Curie temperature of about 628 K, the crystal performs a transition to the orthorhombic r-phase, where the highest permittivity is encountered.4

The physical properties of epitaxial thin films can substantially differ from those in bulk materials. Especially, the two-dimensional clamping can cause considerable strain (compressive or tensile) that may change profoundly the phase transition sequence, the Curie temperature, and permittivity in thin films with respect to the bulk material.^{5,6} In the present work, the question is highlighted whether compressive strain can reduce the Curie temperature in NaNbO₃, for instance, to room temperature and thus lead to an increase of the permittivity of this material. For this purpose, NaNbO₃ thin films are grown on (110) oriented NdGaO₃ single-crystalline substrates via liquid-delivery spin metal organic chemical vapor deposition (MOCVD). The choice of the substrate material leads to a pronounced (slightly anisotropic) compressive misfit strain which determines the crystal structure and orientation of the NaNbO₃ film and is expected to cause a strong modification of the ferroelectric properties.

NaNbO₃ films with thickness up to 80 nm are deposited via MOCVD at a temperature of 700 °C (for details, see Ref. 7). At room temperature, the crystal structure of the substrate $NdGaO_3$ is orthorhombic $(a_{NGO} = 0.5428 \text{ nm},$ $b_{NGO} = 0.5498 \text{ nm}, c_{NGO} = 0.7709 \text{ nm})^8 \text{ and the } (110)$ surface exhibits a nearly squared in-plane lattice with lattice parameters 2×0.3855 nm and 2×0.3863 nm in [001] and [110] direction, respectively. In this paper, the parameters a, b, and c denote orthorhombic lattice parameters, while the index pc indicates the pseudocubic system of NaNbO₃. The orthorhombic unit cell lattice parameters of the antiferroelectric phase of NaNbO₃ at room temperature are a_{NNO} $= 0.55687 \,\mathrm{nm}, \, b_{\mathrm{NNO}} = 1.5523 \,\mathrm{nm}, \, \mathrm{and} \, c_{\mathrm{NNO}} = 0.55047 \,\mathrm{nm},$ which for simplicity is often presented in pseudocubic notation with the corresponding pseudocubic lattice parameters $a^{pc}_{NNO} = 0.3938 \,\text{nm}$, $b^{pc}_{NNO} = 0.3881 \,\text{nm}$, and c^{pc}_{NNO} = 0.3892 nm. Due to energy minimization, NaNbO₃ is expected to grow with the smallest possible distortion on NdGaO₃ which is the a^{pc}-orientation. The resulting lattice mismatch in bpc- and cpc-direction is compressive, i.e., 0.7% and 0.8%, respectively. 10 The structural properties of the NaNbO₃ films are analyzed via high resolution X-ray diffraction experiments (for more details, see Ref. 7). Although X-ray reciprocal space mappings indicate the onset of partial plastic relaxation of the incorporated compressive strain for the thicker films, the in-plane lattice parameters of all NaNbO₃ films almost match the in-plane unit cell of the substrate. The lattice parameters of the 80 nm thick NaNbO₃ film that is used for the cryoelectronic measurements are $b_{NNO}^{pc} \approx 0.3855 \,\text{nm}$, $c_{NNO}^{pc} \approx 0.3863 \,\text{nm}$, and a_{NNO}^{pc} = 0.3945 nm, respectively. The resulting strain $(a_{bulk} - a_{film})/$ a_{film} is compressive in the plane (0.67% and 0.75% in b- and c-direction, respectively), and tensile out of plane (-0.18%)

In order to investigate the in-plane dielectric properties of the NaNbO₃ films, planar capacitors in form of interdigitated electrodes (IDE) are employed, which are obtained via lift-off lithography technique and deposition of a thin (50 nm) Au layer.¹¹ The IDE is arranged such that the

²Leibniz-Institute for Crystal Growth, Max-Born-Str. 2, D-12489 Berlin, Germany

a) Author to whom correspondence should be addressed. Electronic mail: r.woerdenweber@fz-juelich.de. Telephone: 49-2461-61-2365.

electric field E is oriented along the longer axis, i.e., E/[110]NdGaO₃//[001]_{pc}NaNbO₃. In order to obtain a reliable and large signal, a relatively large gap size $s = 5 \mu m$ is chosen that is compensated by large length $d = 700 \,\mu\text{m}$ of the individual IDE's fingers and a large number of fingers resulting in an effective length of the capacitor of 44.1 mm. As a result, room temperature capacitances of 5.47 pF and \sim 13 pF are obtained for a reference sample (without film) and a sample with an 80 nm thick NaNbO₃ film, respectively. The dielectric properties are analyzed as function of temperature (20 K to 320 K), frequency (20 Hz to 2 MHz), and dc-bias voltage (-30 V to 30 V) using a high precision capacitance meter (HP4278A) and a LCR meter (ST2826A). The in-plane real part of the dielectric constant ε' of the NaNbO₃ films is calculated using a partial capacitance model. 12-14 The model is based on conformal mapping and allows to evaluate the capacitive contribution of all components (esp. substrate and ferroelectric film) of planar structures. The model strictly valid for our geometry is the model of Gevorgian et al. 13 However, due to the geometrical design of the IDE and the large permittivity of the NaNbO₃ films in comparison to that of the substrate, all three models yield nearly identical results. The dielectric loss tangent $\tan \delta = \varepsilon''/\varepsilon'$ of the layer is obtained via correction of the total loss tangent using an identical reference sample without NaNbO3 layer.

Fig. 1 shows the dielectric constant, ε' , and dielectric loss, $\tan \delta$, of an 80 nm thick NaNbO₃ film on (110) NdGaO₃. In contrast to unstrained NaNbO₃ which shows a characteristic sharp peak at the Curie temperature and a nearly constant permittivity of $\varepsilon' \approx 500$ at temperatures below the phase transition at about 628 K (Ref. 4) (see inset of Fig. 1), we observe:

(i) a peak in the temperature dependence of ε' of comparable height ($\varepsilon'_{max} \approx 1400$ for 1.5 kHz) but much broader and with a maximum shifted to a temperature slightly below room temperature (e.g., $T_{max} = 252 \text{ K}$ for 1.5 MHz),

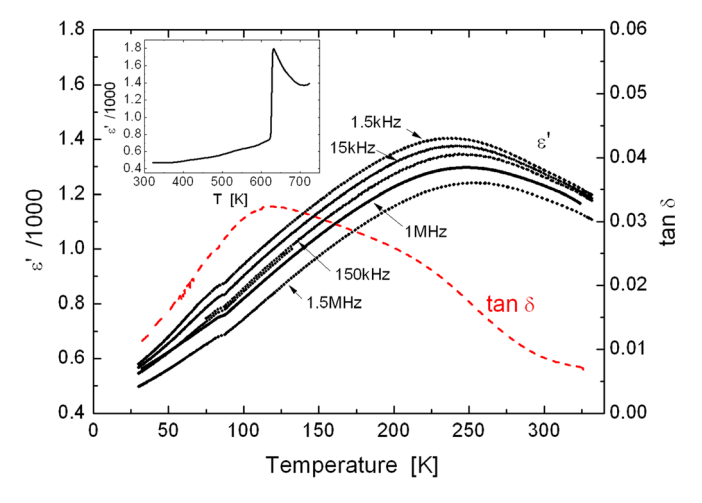


FIG. 1. Permittivity and loss tangents of a NaNbO $_3$ film on (110) NdGaO $_3$ as function of temperature measured for different frequencies (tan δ is only shown for 1 MHz) and an ac-voltage of 1 V. The inset shows the characteristic temperature dependence of the permittivity of unstrained NaNbO $_3$ (single crystal) taken from Ref. 4.

- (ii) a frequency dependence of the permittivity and the temperature of the maximum permittivity T_{max} ,
- (iii) accompanied by losses that are small at room temperature (tan $\delta \approx 0.01$) and increase with decreasing temperature to a maximum of about 0.032 at T \approx 120 K.

It is known that substrate-induced biaxial strain may significantly increase the spontaneous polarization and induce structural, and therefore, ferroelectric phase transitions in a ferroelectric material. These effects not only depend on the amount of strain but also they strongly depend on the direction of the strain (compressive or tensile) and the electric field direction in which the polarization is measured. For example, it has been shown that tensile strain significantly increases T_c for in-plane polarization measurements on $SrTiO_3$ films, whereas compressive strain does not lead to any spontaneous in-plane polarization in the same material.

As demonstrated via X-ray experiments, in our sample, the compressive in-plane strain enforces a monoclinic structure (r-phase) of NaNbO₃ at room temperature.⁷ This symmetry does not exist in the parent bulk compound but is expected to exhibit large dielectric and piezoelectric properties as predicted 16 and experimentally demonstrated 17 for other strained ferroelectric oxides. In agreement with these expectations, our electronic data clearly show a strong enhancement of the permittivity compared to unstrained bulk material⁴ at the regime around room temperature. Moreover, the peak in the ε -vs.-T plot indicates the presence of a phase transition. The broadness of the peak might be caused by the onset of plastic strain relaxation that has been observed for NaNbO₃ films thicker than 10 nm via X-ray analysis. The restricted temperature regime of the measurement and the broadness of the peak do not allow to identify a Curie-Weiss behavior for this transition. In the following, we will discuss the electronic phase (and a possible phase transition) of our strained film and the frequency dependence of the permittivity that indicates a relaxor-type behavior.

A direct test of (anti-)ferroelectricity is provided by permittivity-versus-bias characteristics in Fig. 2. The complete electric field sweeps (Fig. 2(a)) show butterfly-shaped hysteretic curves for all temperatures demonstrating the presence of ferroelectricity. At low temperature, the curves are non-symmetric which represents another indication of the relaxor-type behavior that is discussed below. At higher temperatures, the curves become symmetric and maxima at nonzero bias develop. Comparing the different temperatures, the width of the hysteresis, the position of the maxima, and the tunability seems to be largest for the temperature close to $T_{max} \approx 250 \,\mathrm{K}$ (see Fig. 2(c)), the maximum in the ε' -vs.-T plot. This might be taken for another indication of the ferroelectric phase transition which seems to set in at this temperature, and due to the partial plastic strain relaxation of the film, leads to the broad peak in the temperature dependence of the permittivity.

A detailed analysis of dc electric field sweeps restricted to the positive field range (Fig. 2(b)) shows a first strong increase of permittivity of the virgin material that vanishes already in the second cycle. This effect is also known for unstrained NaNbO₃ which is antiferroelectric in the virgin

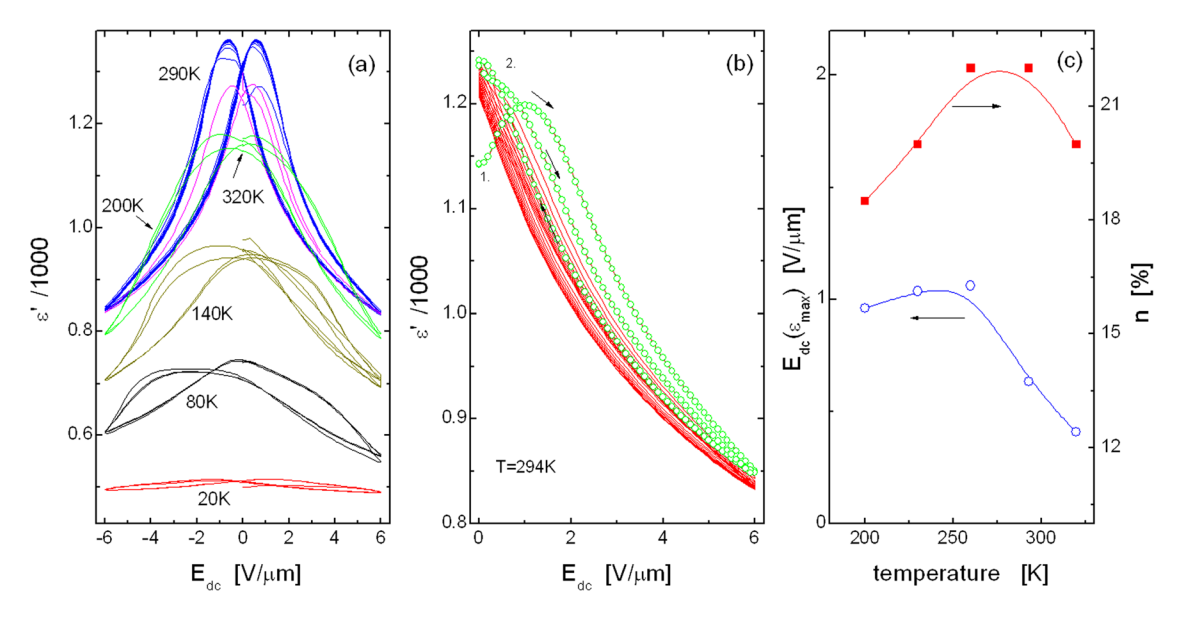


FIG. 2. Dc bias dependence of the permittivity of a NaNbO₃ film on (110) NdGaO₃ measured at 1 MHz for continuous electric field sweeps at different temperatures (a) and for positive electric field sweeps (0 to 6 V/ μ m) at room temperature (b). In (b), the first 1.5 cycles are highlighted by dots, arrows indicating the direction of the sweep and numbers distinguish the starting point of the 1st (virgin) and 2nd cycle. Figure (c) shows the temperature dependence of the dc bias fields of the maxima in $\varepsilon'(E_{dc})$ and the tunability $n = [\varepsilon'(0) - \varepsilon'(E_{dc})]/\varepsilon'(0)$ for $E_{dc} = 6 \text{ V}/\mu$ m that are obtained from figure (a).

state and for which electric polling leads to ferroelectric properties, i.e., already a small applied electric field induces a phase transition from the antiferroelectric to the ferroelectric phase. Moreover, the width of the hysteresis decreases with increasing numbers of cycles. The latter observation and the frequency dependence of the permittivity point towards a relaxor type behavior that has also been reported for other strained ferroelectric materials. 11

Finally, we discuss the frequency dependence of the permittivity which is an indication for a relaxor-type ferroelectric behavior. For a relaxor ferroelectric phase, characteristic features should be observable especially at the transition to the relaxor ferroelectric state, i.e., at the maximum in the ε' -versus-T plot. The inset of Fig. 3 shows the temperature dependence of the permittivity for different frequencies. Especially, at the peak in ε' , large differences in the permittivity are recorded for different frequencies. With decreasing frequency, the permittivity

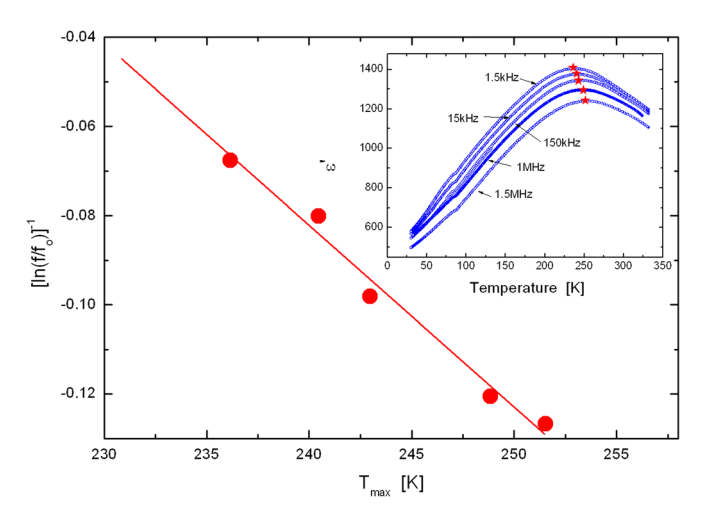


FIG. 3. Vogel-Fulcher equation fit according to Eq. (1) using an attempt frequency of f_o = 4 GHz. The inset shows the temperature dependence of the permittivity for different frequencies, the maxima are indicated by symbols.

increases and the temperature of the maximum T_{max} decreases. This behavior is characteristic for many relaxor ferroelectrics, 20,21 it is described by the Vogel-Fulcher equation 22

$$f = (2\pi\tau_o)^{-1} \exp\left[-\frac{E_a}{k_B(T_{\text{max}} - T_{VF})}\right],$$
 (1)

with the attempt frequency $f_o = (2\pi\tau_o)^{-1}$, the activation energy E_a , Boltzmann constant k_B , and the static freezing temperature T_{VF} .

A Vogel-Fulcher equation fit of our permittivity data measured for frequencies ranging between 1.5 kHz and 1.5 MHz is given in Fig. 3. It demonstrates the predicted linear relation between the reduced frequency $[\ln(f/f_o)]^{-1}$ and T_{max} . Inserting a reasonable value $f_o = 4$ GHz for the attempt frequency yields $T_{VF} = 219.7$ K and $E_a = 21.2$ meV for the static freezing temperature and activation energy, respectively. The evaluated activation energy value represents a typical value for an activation energy of a relaxor ferroelectric. 20,23

In summary, we demonstrated that the lattice mismatch between (110) oriented NdGaO₃ substrates and NaNbO₃ films leads to significant modifications of structural and ferroelectric properties of the NaNbO₃ films. The slightly anisotropic compressive in-plane strain in the NaNbO₃ film leads to a low symmetry monoclinic or triclinic r-phase with reduced in-plane parameters $(b^{pc}_{NNO} \approx 0.3855 \text{ nm},$ $c_{NNO}^{pc} \approx 0.3863 \, \text{nm}$) and an expanded out-of-plane lattice parameter ($a^{pc}_{NNO} = 0.3945 \text{ nm}$). As a consequence, the inplane permittivity and tunability are strongly enhanced (e.g., $\varepsilon' \approx 1250$ and n(6 V/ μ m) $\approx 21\%$ in c^{pc}-direction, at room temperature and 1 MHz). Furthermore, the broad peak in the temperature dependence of the in-plane permittivity is indicative for the onset of a phase transition at about 250 K. Although the broadness of the peak does not allow to identify a Curie-Weiss behavior for this transition it might be of advantage for applications, since the permittivity stays large for a large temperature regime. The antiferroelectric phase is easily suppressed, already small applied electric fields induce a phase transition from the antiferroelectric to the ferroelectric phase. The (anti-)ferroelectric phase shows relaxor behavior, i.e., permittivity and the maxima in the permittivity are frequency dependent. In general, it is demonstrated that NaNbO₃ represents an ideal candidate for "strain engineering" of structural and ferroelectric properties.

The authors would like to thank A. Offenhäusser, R. Kutzner, T. Grellmann, K. Greben, T. Ehlig, and S. Markschies for their valuable support.

- ¹Y. Saito, H. Takao, T. Tani, T. Nonoyama, K. Takatori, T. Homma, T. Nagaya, and M. Nakamura, Nature **432**, 84 (2004).
- ²Y. I. Yuzyuk, R. A. Shakhovoy, S. I. Raevskaya, I. P. Raevski, M. El Marssi, M. G. Karkut, and P. Simon, Appl. Phys. Lett. **96**, 222904 (2010); V. Lingwal and N. S. Panwar, J. Appl. Phys. **94**, 4571 (2003); S. K. Mishra, N. Choudhury, S. L. Chaplot, P. S. R. Krishna, and R. Mittal, Phys. Rev. B **76**, 024110 (2007).
- ³A. M. Glazer and H. D. Megaw, Acta Crystallogr. A **29**, 489 (1973); J. Dec, Cryst. Res. Technol. **18**, 195 (1983).
- ⁴G. Shirane, R. Newnham, and R. Pepinsky, Phys. Rev. **96**, 581–588 (1954).
- ⁵J. H. Haeni, P. Irvin, W. Chang, R. Uecker, P. Reiche, Y. L. Li, S. Choudhury, W. Tian, M. E. Hawley, B. Craigo, A. K. Tagantsev, X. Q. Pan, S. K. Streiffer, L. Q. Chen, S. W. Kirchoefer, J. Levy, and D. G. Schlom, Nature 430, 758 (2004).
- ⁶R. Wördenweber, E. Hollmann, R. Kutzner, and J. Schubert, J. Appl. Phys. 102, 044119 (2007).
- ⁷J. Schwarzkopf, M. Schmidbauer, T. Remmele, A. Duk, A. Kwasniewski, S. Bin Anooz, A. Devi, and R. Fornari, J. Appl. Crystallogr. **45**, 1015 (2012).

- ⁸M. Schmidbauer, A. Kwasniewski, and J. Schwarzkopf, Acta Cryst. B 68, 8–14 (2012).
- ⁹M. C. Morris, H. F. McMurdie, E. H. Evans, B. Paretzkin, H. S. Parker, N. C. Panagiotopoulos, and C. R. Hubbard, "Standard X-ray diffraction powder patterns," Natl. Bur. Stand. (U.S.) Monograph No. 18 (National Bureau of Standards, Gaithersburg, 1981).
- 10 The lattice mismatch is calculated using $\Delta a/a = (a_{\rm NNO} a_{\rm NGO})/a_{\rm NGO}$ for the different orientations of the film, where $a_{\rm NNO}$ and $a_{\rm NGO}$ describe the pseudocubic lattice parameters of the film and the substrate material, respectively.
- ¹¹R. Wördenweber, J. Schubert, T. Ehlig, and E. Hollmann, J. Appl. Phys. 113, 164103 (2013).
- ¹²O. G. Vendik, S. P. Zubko, and M. A. Nikol'skii, Tech. Phys. **44**, 349–355 (1999); O. G. Vendik and M. A. Nikol'skii, *ibid*. **46**, 112–116 (2001).
- ¹³S. S. Gevorgian, T. Martinsson, P. L. Linner, and E. L. Kollberg, IEEE Trans. Microwave Theory Tech. 44, 896 (1996).
- ¹⁴E. Chen and S. Y. Chou, IEEE Trans. Microwave Theory Tech. **45**, 939 (1997)
- ¹⁵N. A. Pertsev, A. G. Zembilgotov, and A. K. Tagantsev, Phys. Rev. Lett. 80, 1988 (1998); N. A. Pertsev, V. G. Kukhar, H. Kohlstedt, and R. Waser, Phys. Rev. B 67, 054107 (2003).
- ¹⁶Q. Y. Qiu, S. P. Alpay, and V. Nagarajan, J. Appl. Phys. **107**, 114105 (2010).
- ¹⁷G. Catalan, A. Janssens, G. Rispens, S. Csiszar, O. Seeck, G. Rijnders, D. H. A. Blank, and B. Noheda, Phys. Rev. Lett. 96, 127602 (2006); M. D. Nguyen, M. Dekkers, E. Houwman, R. Steenwelle, X. Wan, A. Roelofs, T. Schmitz-Kempen, and G. Rijnders, Appl. Phys. Lett. 99, 252904 (2011).
- ¹⁸L. E. Cross and B. J. Nicholson, Philos. Mag. **46**, 453 (1955).
- ¹⁹A. A. Bokov and Z.-G. Ye, Solid State Commun. **116**, 105 (2000).
- ²⁰D. Viehland, S. J. Jang, L. E. Cross, and M. Wuttig, J. Appl. Phys. 68, 2916 (1990).
- ²¹A. A. Bokov and Z.-G. Ye, J. Mater. Sci. **41**, 31–52 (2006).
- ²²H. Vogel, Phys. Z **22**, 645 (1921); G. S. Fulcher, J. Am. Ceram. Soc. **8**, 339 (1925).
- ²³H. W. Jang, A. Kumar, S. Denev, M. D. Biegalski, P. Maksymovych, C. W. Bark, C. T. Nelson, C. M. Folkman, S. H. Baek, N. Balke, C. M. Brooks, D. A. Tenne, D. G. Schlom, L. Q. Chen, X. Q. Pan, S. V. Kalinin, V. Gopalan, and C. B. Eom, Phys. Rev. Lett. 104, 197601 (2010).